JOURNAL OF MATERIALS SCIENCE 16 (1989) 2255–2261

Rubber toughening of plastics

Part 12 *Deformation mechanisms in toughened nylon 6,6*

CLIVE B. BUCKNALL, PATRICIA S. HEATHER*, ANDREA LAZZERI†
School of Industrial Science, Cranfield Institute of Technology, Cranfield, Bedford MK43 OAL, UK

The tensile behaviour of a rubber-toughened polyamide 6,6 (RTPA66) is compared with that of the corresponding untoughened polyamide (PA66). At constant strain rate, moisture-conditioned specimens of RTPA66 show a substantial increase in volume ΔV with increasing extension ε, whereas PA66 becomes denser. At ε = 40%, ΔV is 6% in RTPA66, but −1.4% in PA66. In creep experiments on both polymers, extension follows the Andrade equation $\varepsilon(t) = \varepsilon(0) + bt^{1/3}$. Eyring plots of log b against applied stress σ are linear for the PA66, but the RTPA66 shows a sharp increase in $d \log b/d\sigma$ above 30 MPa, where significant dilatation begins. Scanning electron micrographs of tensile and impact specimens reveal that dilatation in RTPA66 is due to formation of voids within the rubber particles, leading to fibrillation of the nylon matrix at high strains. It is concluded that this cavitation accelerates shear yielding in the nylon matrix.

1. Introduction

Toughened nylons (polyamides) are now well established commercially as engineering polymers. Addition of about 20 wt % of a suitable rubber in the form of small particles greatly increases the impact resistance of nylons [1–6], which are especially notch-sensitive when they are dry. The rubbers must have sufficient resistance to oxidation to be able to withstand the high barrel temperatures used to mould nylons. Of the many different types of elastomers that have been tested as toughening agents for nylons, ethylene-propylene (EP) copolymers are amongst the most successful. The EP rubbers are treated with maleic anhydride to provide reactive sites along the chain, and then melt-blended with nylon. Reactions between terminal amine groups on the nylon and the anhydride groups bonded to the EP rubber chain produce graft copolymers which aid dispersion and enhance interfacial adhesion [2, 5].

The present paper compares one such toughened nylon, based on nylon 6,6, with the untoughened parent polymer. The techniques used are similar to those employed in previous studies in this series: longitudinal and lateral strains are measured in order to obtain quantitative information about the mechanisms and kinetics of tensile deformation. In this respect, the ductility of the parent polymer is a distinct advantage, since it permits an extensive characterisation of creep behaviour in the untoughened polymer.

2. Experimental details

2.1. Materials

Two commercial grades of nylon were used for this work: an unmodified PA66, and a rubber-toughened material containing 20 wt % of a maleinated olefin rubber, as described above. Both materials were dried under vacuum for 16 h at 105° C before being moulded into three types of specimen: (a) edge-gated circular discs having a diameter of 75 mm and a thickness of 3 mm; (b) square plaques measuring 120 × 120 × 6 mm^3; and (c) ASTM tensile bars. The barrel and mould temperatures were 270 and 90° C respectively. After moulding, the discs were conditioned for a minimum of 6 weeks at 20 ± 1° C and 60% RH before being tested.

2.2. Methods

Dumb-bell creep specimens having a parallel gauge portion 5 mm wide and 30 mm long were milled from the injection-moulded discs. The overall specimen dimensions meant that it was possible to obtain only one creep specimen from each disc. Tensile creep tests were carried out at 20° C and 60% RH using extensometers to determine elongation and lateral strain, from which volume strain ΔV was calculated [7–10].

Tensile tests at constant strain rate were carried out at 23° C on an Instron tensometer, using injection moulded tensile bars with a 70 mm gauge length and a 3 × 13 mm^2 cross section. The crosshead speed was 5 mm min^{-1}. Volume changes were again monitored throughout each test, using contact extensometers.

Charpy impact tests were carried out over a range of temperatures, using a Ceast instrumented impact testing system, with a falling-weight loading frame designed and built at Cranfield. Specimens measuring 120 × 25 × 6 mm^3 with a span of 100 mm were machined from injection moulded plaques. A central sharp vee notch was cut to a depth of between 10 and

* *Present address:* Polysar Nederland B V, Postbus 5024, 6800 Arnhem, The Netherlands.
‡ *Present address:* Department of Chemical Engineering, CNR Polymer Center, Via Diotisalvi 2, University of Pisa, Italy.

0022–2461/89 $03.00 + .12

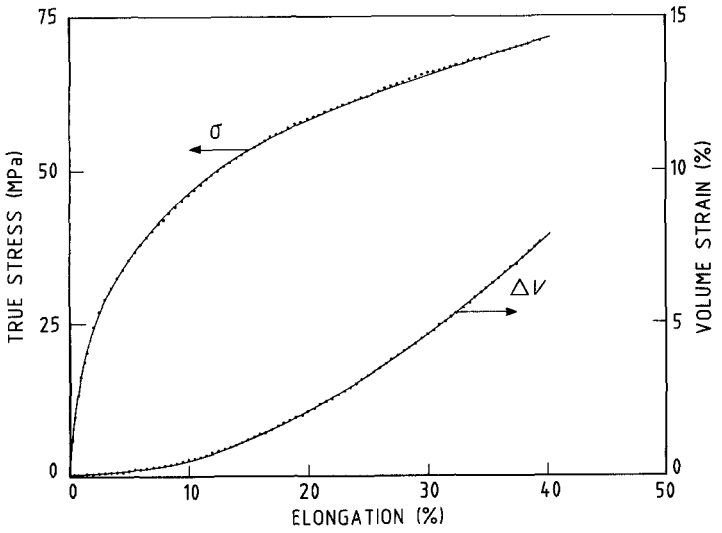

Figure 1 Tensile dilatometry curve for conditioned PA66 at 23° C. Strain rate 0.12% sec^{-1}. (0% EPR)

11 mm, and extended a further 2 mm with a fresh razor blade, to give $a/W \approx 0.5$. The striker height was set at 20 cm, so that the impact velocity was 2.0 m sec^{-1}. Specimens were cooled to the test temperature for a period of at least 30 min before testing.

Specimens for scanning electron microscopy were prepared from previously drawn material by fracturing at liquid nitrogen temperatures: tensile and Charpy bars were cold-fractured both parallel and normal to the draw direction. The fracture surfaces were coated with Au–Pd prior to examination.

3. Results

Curves of true stress against elongation for the two polymers in tests at constant rate of extension are compared in Figs 1 and 2. At $\varepsilon > 40\%$, the PA66 necks to about one third of its original cross-sectional area, and the neck then propagates along the gauge length. For this reason, only data obtained below $\varepsilon = 40\%$ are included in Fig. 1. The neck region is slightly less translucent than the remainder of the specimen, but the change in opacity is not sufficient to be described as stress-whitening. By contrast, the RTPA66 draws uniformly in the gauge length, without a localized reduction in cross-sectional area, and becomes progressively and densely whiter as the strain increases. The toughened polymer shows an increase in volume as it extends, $dV/d\varepsilon$ reaching 0.20 at strains above 20%. Under the same conditions, unmodified nylon undergoes a progressive decrease in volume.

Isochronous creep tests show that rubber toughening significantly reduces the modulus of the nylon, as illustrated in Fig. 3. Both the toughened and untoughened polymers begin to drop in modulus at strains of about 0.5%, and the non-linearity becomes pronounced at strains above 1%.

Standard creep curves for PA66 and RTPA66 at 30 MPa are compared in Fig. 4. Although the strains reached are different, the pattern of behaviour is similar in the two materials: after the initial elastic response to loading, the specimen extends at a decreasing rate, the extension being matched by a decrease in cross-sectional area ΔA, so that the volume strain ΔV remains effectively constant. This pattern of creep behaviour was observed in all of the creep tests carried out on the untoughened polymer PA66, over the stress range 10 to 40 MPa. By contrast, creep of the toughened material RTPA66 shows a change above 30 MPa; at higher stresses, the volume strain increases steadily with time during the test. This change in deformation mechanism with applied stress is emphasized in Fig. 5, in which $\Delta V(t)$ is plotted against $\varepsilon(t)$. At 40 MPa, the slope of the line is 0.41, showing that dilatational processes make a substantial contribution

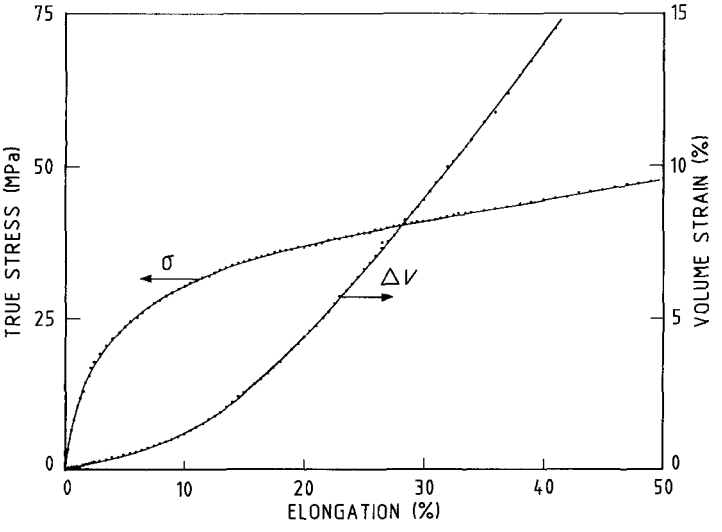

Figure 2 Tensile dilatometry curve for conditioned RTPA66 at 23° C. Strain rate 0.12% sec^{-1}. (20% EPR).

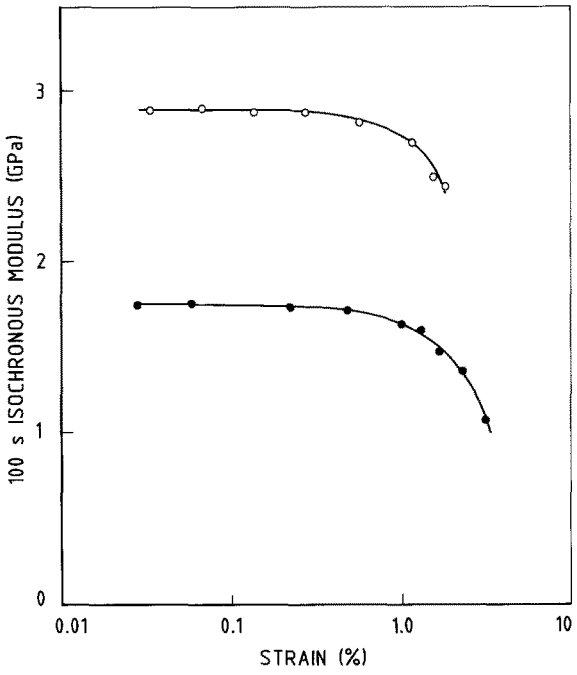

Figure 3 Isochronous creep modulus at 100 sec on conditioned PA66 (○) and RTPA66 (●) at 20° C.

to the total extension in RTPA66 at moderately high stresses and strain rates. The slope $dV/d\varepsilon$ is higher than that obtained from the constant strain rate test at $\varepsilon > 20\%$.

In both toughened and untoughened PA66, the creep curves can be fitted to the Andrade equation

$$\varepsilon(t) = \varepsilon(0) + bt^{1/3} \quad (1)$$

where the rate coefficient b is a function of stress and temperature. Plots of $\varepsilon(t)$ against $t^{1/3}$ for the two polymers are presented in Figs 6 and 7. The relationship between applied stress σ and the parameter b determined from these curves is shown in Fig. 8. The PA66 follows a simple Eyring relationship of the form

$$b = Q \exp(\gamma v\sigma/k_B T) \quad (2)$$

where Q is a constant, γ a stress concentration factor, v the activation volume for the deformation process, k_B Boltzmann's constant, and T the temperature. On the assumption that $\gamma = 1$ in the absence of rubber particles or other stress-concentrating additives, the data give a value of $v = 1.04\,nm^3$ for PA 66.

Between 10 and 30 MPa, the rubber-toughened PA66 behaves in a similar manner to unmodified PA66, following Equation 2, but with a slightly increased slope. A simple explanation of this result is that the same deformation mechanisms operate in both materials, with the same value of activation volume, v, and that the higher slope is due to an increased stress concentration factor. On this basis, the estimated value of γ in the RTPA66 is 1.35. This factor also accounts for the increase in b over the stress range; it is not necessary to invoke an increase in the pre-exponential factor Q.

Above 30 MPa, the relationship between log b and σ changes abruptly. The data show a satisfactory fit to Equation 2, but the slope $\gamma v/k_B T$ increases by a factor of 3.2. As this change coincides with the onset of cavitation, as shown by the volumetric data, it must be concluded that the two phenomena are connected.

Scanning electron micrographs of fractured tensile specimens are shown in Figs 9 and 10. They reveal a pattern of dispersed voids in RTPA66 which is not seen in PA66 itself. At $\varepsilon = 40\%$, the voids are roughly spherical, and approximately 0.3 μm in diameter. As the strain increases, they become highly elongated in the draw direction, but show relatively little change in lateral dimensions. Many of the voids contain small fibrils, which in general lie approximately perpendicular to the draw direction. No corresponding pattern of voids could be found in tensile specimens of the unmodified nylon, as expected in view of the extensometer data.

Notched Charpy tests on the RTPA66 over a range of temperatures showed a sharp increase in fracture energy, accompanied by full whitening of the fracture surface, at temperatures above −20° C. A comparison of impact data for the toughened and untoughened polymers is presented in Fig. 11. Charpy specimens from room temperature tests on RTPA66 were cryogenically fractured in the plane normal to the fracture surface, and examined in the scanning electron microscope. As shown in Fig. 12, this procedure revealed extensive drawing of the nylon, and formation of

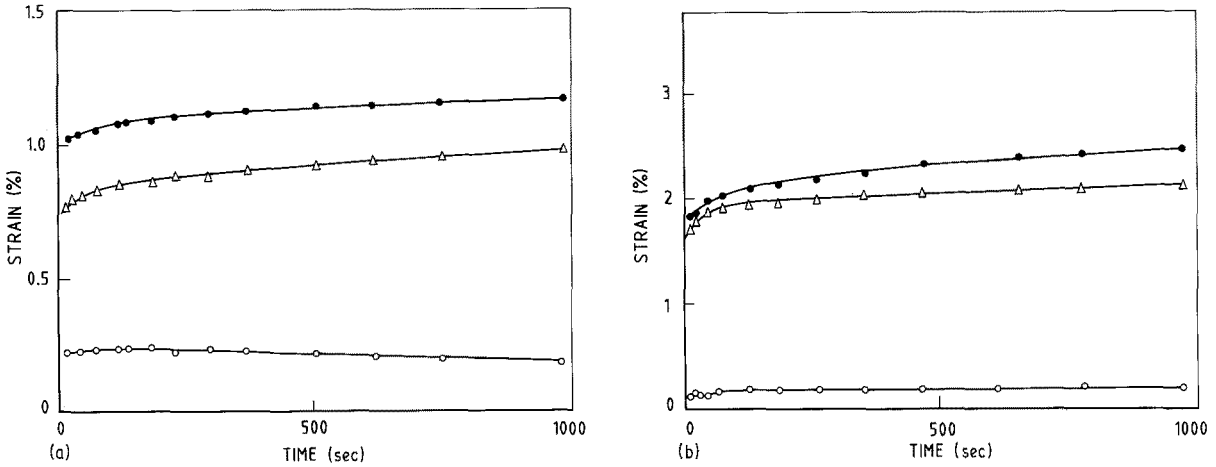

Figure 4 Creep curves showing total extension ε (●), area strain $-\Delta A$(△) and volume strain ΔV(○) for conditioned PA66 at 20° C and 30 MPa. (a) PA66; (b) RTPA66.

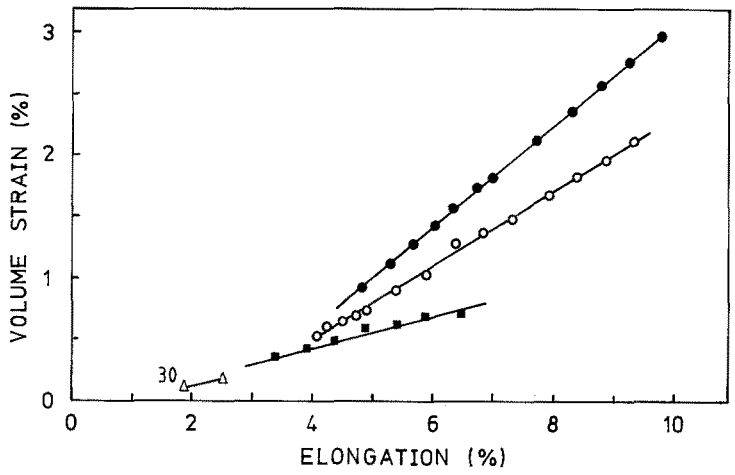

Figure 5 Relationship between volume strain and elongation in conditioned RTPA66 over a range of stresses. (● 40 MPa, ○ 38 MPa, ■ 34 MPa).

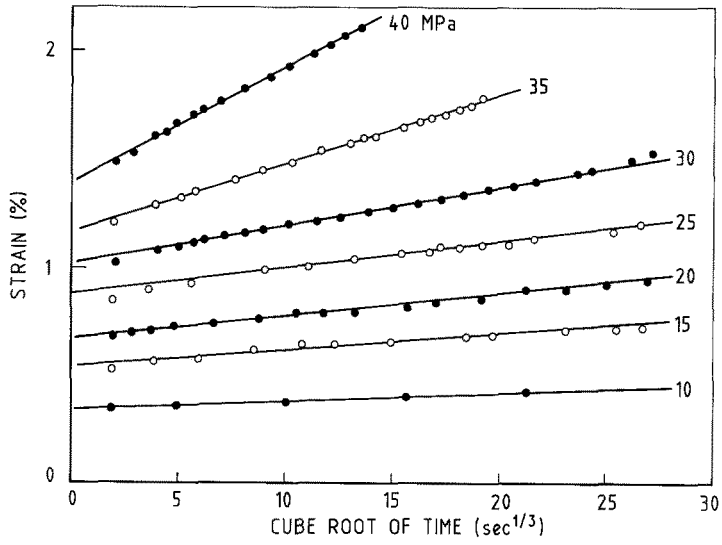

Figure 6 Andrade plots of creep data for PA66 at 20° C.

elongated voids, which was most marked in the stress-whitened zone.

There was no evidence for crazing in any of the specimens studied. The main effect of void formation at all test speeds appears to be an acceleration of shear yielding mechanisms in the nylon matrix.

4. Discussion

This work has shown that volume changes make a significant contribution to tensile deformation in toughened nylon 6,6. Electron microscopy reveals a random pattern of small voids in strained specimens of the rubber-toughened polymer. By contrast, the unmodified nylon shows a progressive slow decrease in volume with increasing tensile strain, which is probably due to an increase in crystallinity within shear zones. A similar increase in density presumably occurs within the shear bands in RTPA66, which means that the measured values of ΔV underestimate the amount of voiding occurring in the toughened polymer.

Cavitation initiated by rubber particles is well known in toughened non-crystalline polymers [11–13].

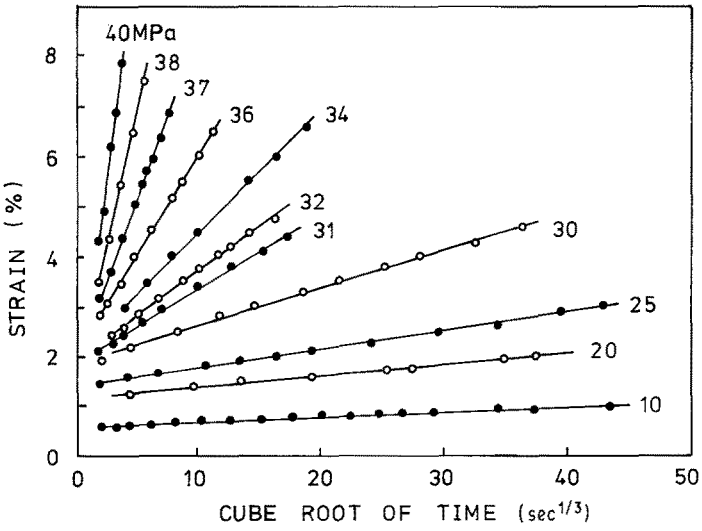

Figure 7 Andrade plots of creep data for RTPA66 at 20° C.

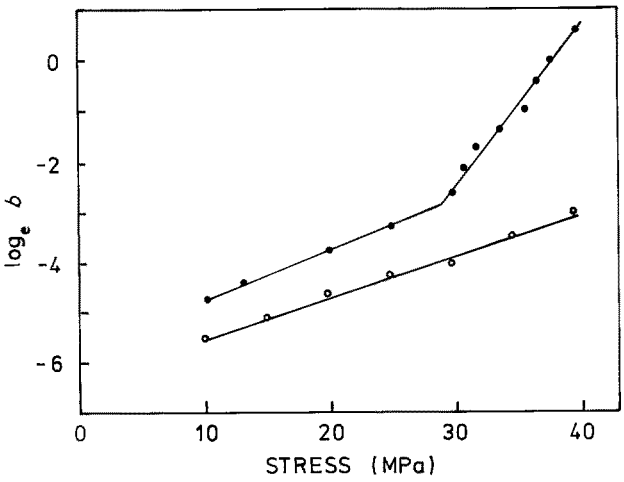

Figure 8 Eyring plots of log b against applied stress σ. (● RTPA66, ○ PA66).

In semi-crystalline polymers, it has been observed in impact specimens of toughened poly(butylene terephthalate) (TPBT) by Polato [14], in tensile specimens of toughened nylon 6,6 by Ramsteiner and Heckmann [15] and in toughened nylon 6 by Borggreve *et al.* [6, 16]. None of these authors observed crazing.

The present work confirms the observations of Ramsteiner and Heckmann on RTPA66. The rubber particles initate voiding either internally or at the rubber–matrix boundary, and the voids then elongate as the specimen extends. The number of voids increases with strain, so that they eventually become interconnected, producing nylon fibrils approximately 0.2 μm in diameter stretched parallel to the draw direction. Finally, the fibrils begin to break, and fracture of the whole specimen follows.

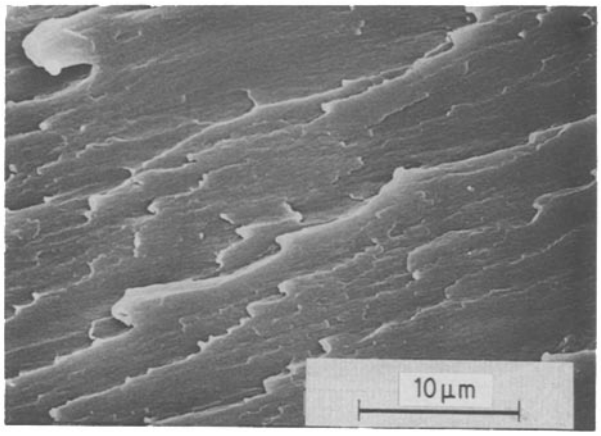

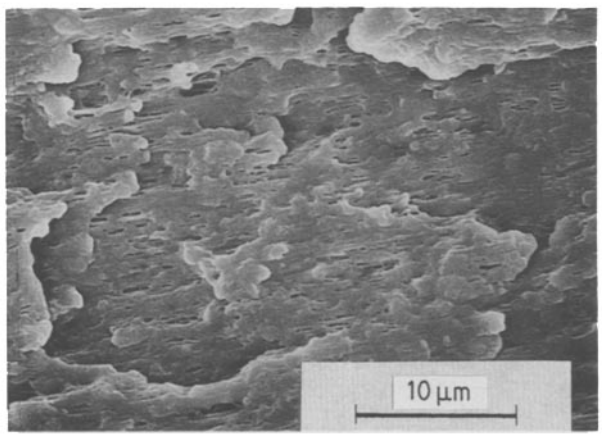

Figure 9 Scanning electron micrographs of specimens tested in tension at 23° C to 80% strain, and fractured at cryogenic temperatures in plane parallel to the tensile axis: (a) PA66; (b) RTPA66.

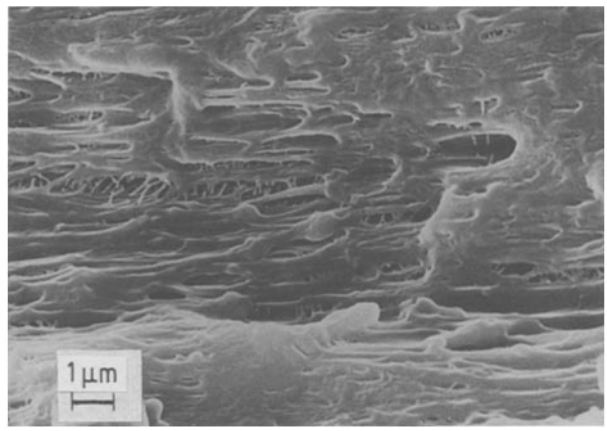

Figure 10 Higher magnification view of RTPA66 tensile specimen as shown in Fig. 9b. Note fibrillar material within cavities.

Very little voiding occurs at low stresses and strains. There is an initial increase in volume due to the hydrostatic component of stress, P_H, which is given by $\sigma/3$, where σ is the applied tensile stress. However, the principal mechanism of extension at this stage is shear deformation, which is essentially a constant-volume process. In RTPA66 the creep behaviour changes abruptly when the tensile strain reaches 4% and the applied stress exceeds 30 MPa, corresponding to a hydrostatic tension $P_H = 10$ MPa.

The value of 10 MPa for the hydrostatic tension P_H at which cavitation begins may be compared with the cavitation stress of $P_H = 5E/6$ predicted by Gent and Lindley [17] for a rubber of Young's modulus E. In experiments on rubber samples mounted between metal surfaces, Cho and Gent obtained values of P_H/E between 0.7 and 3.8, depending on the shape of the constraining surfaces [18]. On this basis, the critical tensile stress for voiding during creep would indicate a modulus between 3 and 15 MPa for the rubber, in reasonable agreement with the known properties of unfilled and lightly crosslinked EPR.

Both before and after the initiation of dilatation, creep strain follows Andrade creep kinetics to a good approximation. In this respect, nylons behave in a similar way to a number of other polymers in which shear yielding is the dominant mode of deformation. Others forms of empirical power law relationship between ε and t could perhaps give a somewhat better fit to the experimental data. However, they do not provide a significant improvement over the Andrade equation for present purposes, namely, to provide a convenient basis for defining rate coefficients in terms of the parameter b, which can be related to the structure of the polymer.

Plots of log b against σ for PA66 give a straight line, in accordance with the Eyring model for stress-activated flow. Addition of 25 vol. % of rubber particles raises b, and results in a small increase in d log b/dσ over the lower range of applied stresses, where shear yielding is the predominant mechanism of deformation. At stresses above 30 MPa, both Andrade kinetics

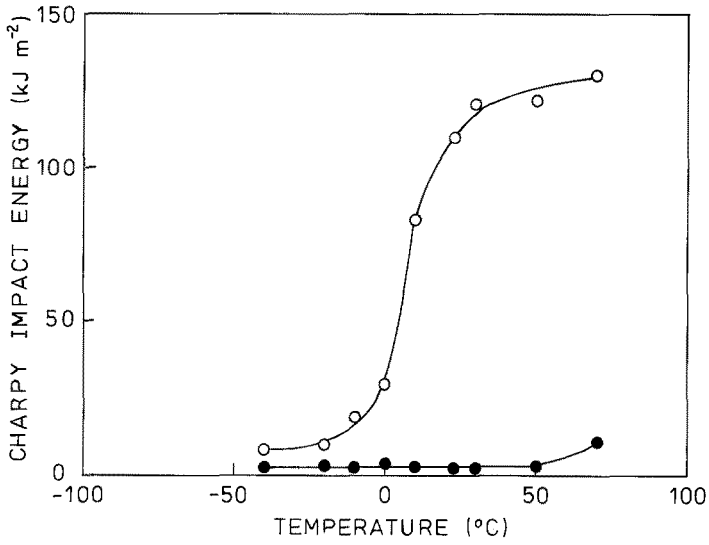

Figure 11 Charpy impact data on sharply-notched bars of PA66 (●) and RTPA66 (○) tested over a range of temperatures.

and the Eyring equation still apply to RTPA66, but d log b/dσ increases sharply as the cavitation mechanism begins to contribute to deformation.

The change in slope is not due simply to the additional strain introduced by the volume increase. At its maximum in creep tests, $dV/d\varepsilon = 0.42$; in other words, voiding has the effect of increasing strain increments by about 70%, as compared with shear yielding alone. A corresponding increase of the strain rate would not be sufficient to cause the marked change in d log b/dσ shown in Fig. 8. Nor would it account for the increase in log b with stress.

Another possibility is that the voids act effectively as additional rubber particles, increasing the rate of initiation of shear bands. However, a large increase in rate occurs at very small volume strains ΔV, and it is, therefore, clear that the effects of void formation cannot be attributed to a small increase equal to ΔV in the effective volume fraction of rubber particles.

An explanation which is consistent with the experimental observations is that the formation of voids results in a change not simply in the magnitude but also in the form of the stress tensor in the material surrounding the growing shear bands. Cavitation of the rubber particles will result in a local decrease in the hydrostatic component of stress, and a corresponding increase in the deviatoric component. Since the deviatoric component is the controlling stress term in the Eyring equation (Equation 2), as applied to shear yielding in nylon, this change in stress state due to void formation should result in an increase in γ.

As has been noted in previous studies of deformation kinetics in rubber-toughened plastics [9, 10], stress concentration factors are relatively low when shear-yielding is the dominant deformation mechanism, indicating that the rate-controlling step does not occur near the rubber particles, where γ is high, but at some distance from the particle. This suggests that initiation of shear bands is relatively rapid, and that growth, which is much slower, constitutes the rate-controlling step.

Several different models have been proposed to explain the toughness of rubber-modified nylons, and the effects of particle size on impact properties. Hobbs *et al.* [3] and Wu [4, 19] suggest that optimum performance is achieved when the rubber particles are sufficiently close to enable stress fields of neighbouring particles to overlap. However, Borggreve *et al.* [6, 16] question this explanation, noting that interparticle spacing controls the brittle–ductile transition temperature even when the rubber content is small and stress-field overlap is negligible.

Clearly, further work is needed to clarify the relationship between particle size and impact properties. The present work has shown that cavitation within the rubber particles causes a substantial change in the kinetics of deformation in nylon 6,6, and provides a basis for treating other aspects of toughening in terms of kinetics.

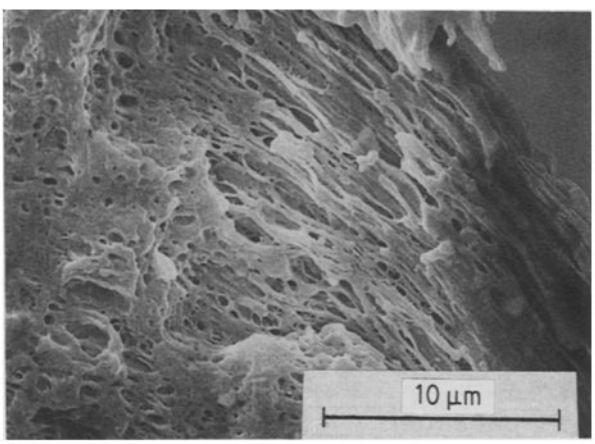

Figure 12 Scanning electron micrograph showing cavitation and drawing near the fracture surface of an RTPA66 Charpy bar tested at 23° C. Specimen preparation as for Fig. 9.

Acknowledgements

The authors thank ICI for a grant in support of this work, and P. Narducci of the University of Pisa for assistance with scanning electron microscopy.

References

1. E. A. FLEXMAN, *Polym. Eng. Sci.* **19** (1979) 564.
2. U S Patent 1 552 352 (1979).
3. S. Y. HOBBS, R. C. BOPP and V. H. WATKINS, *Polym. Eng. Sci.* **23** (1983) 380.
4. S. WU, *J. Polym. Sci. Phys. Edn* **21** (1983) 699.
5. S. CIMMINO, L. D'ORAZIO, R. GRECO, M. MALINCONICO, C. MANCARELLA, E. MARTUSCELLI,

R. PALUMBO and G. RAGOSTA, *Polym. Eng. Sci.* **24** (1984) 48.
6. R. J. M. BORGGREVE, R. J. GAYMANS, J. SCHUIJER and J. F. INGEN-HOUSZ, *Polymer* **28** (1987) 1489.
7. C. B. BUCKNALL and D. CLAYTON, *J. Mater. Sci.* **7** (1972) 202.
8. C. B. BUCKNALL and I. C. DRINKWATER, *ibid.* **8** (1973) 1800.
9. C. B. BUCKNALL and C. J. PAGE, *ibid.* **17** (1982) 808.
10. C. B. BUCKNALL, I. K. PARTRIDGE and M. V. WARD, *ibid.* **19** (1984) 2064.
11. H. BREUER, F. HAAF and J. STABENOW, *J. Macromol. Sci. Phys.* **B14** (1977) 387.
12. A. F. YEE and R. A. PEARSON, *J. Mater. Sci.* **21** (1986) 2462.
13. *Idem, ibid.* **21** (1986) 2475.
14. F. POLATO, *ibid.* **20** (1985) 1455.
15. F. RAMSTEINER and W. HECKMANN, *Polym. Commun.* **26** (1985) 199.
16. R. J. M. BORGGREVE, PhD Thesis, University of Twente, Netherlands (1988).
17. A. N. GENT and P. B. LINDLEY, *Proc. R. Soc.* **A249** (1969) 2520.
18. K. CHO and A. N. GENT, *J. Mater. Sci.* **23** (1988) 141.
19. S. WU, *Polymer* **26** (1985) 1855.

Received 20 May
and accepted 15 August 1988